CONF-810806--8

MASTER

EXPERIMENTAL INVESTIGATIONS OF TWO-PHASE MIXTURE LEVEL SWELL AND AXIAL VOID FRACTION DISTRIBUTION UNDER HIGH PRESSURE, LOW HEAT FLUX CONDITIONS IN ROD BUNDLE GEOMETRY*

T. M. Anklam

Oak Ridge National Laboratory
Oak Ridge, Tennessee 37830
(615) 574-0772

M. D. White

Oak Ridge National Laboratory
Oak Ridge, Tennessee 37830
(615) 574-0764

ABSTRACT

Experimental data is reported from a series of quasi-steady-state two-phase mixture level swell and void fraction distribution tests. Testing was performed at Oak Ridge National Laboratory in the Thermal Hydraulic Test Facility – a large electrically heated test loop configured to produce conditions similar to those expected in a small break loss of coolant accident. Pressure was varied from 2.7 to 8.2 MPa and linear power ranged from 0.33 to 1.95 kW/m. Mixture swell was observed to vary linearly with the total volumetric vapor generation rate over the power range of primary interest in small break analysis. Void fraction data was fit by a drift-flux model and both the drift-velocity and concentration parameter were observed to decrease with increasing pressure.

*Research sponsored by Division of Reactor Safety Research, U.S. Nuclear Regulatory Commission under Interagency Agreements DOE 40-551-75 and 40-552-75 with the U.S. Department of Energy under contract W-7405-eng-26 with the Union Carbide Corporation.

Introduction and Theory

In recent years considerable effort has been directed toward the study of nuclear reactor thermal hydraulics under high pressure, low heat flux conditions; conditions which are postulated to occur in a small break loss of coolant accident. Under sponsorship of the U.S. Nuclear Regulatory Commission, Oak Ridge National Laboratory (ORNL) has experimentally investigated thermal hydraulics under conditions similar to those expected in a small break loss of coolant accident. This paper presents the results of a series of quasi-steady-state, steam-water experiments designed to acquire axial void fraction distributions and mixture level swell measurements.

Figure 1 is a schematic of a nuclear reactor subchannel in a partially uncovered configuration. The subchannel can be divided into three primary thermal hydraulic regions: (1) a subcooled or saturated inlet region, (2) a saturated boiling region, and (3) a high quality or dry steam cooling region. Because of the low heat fluxes associated with decay heat levels, the subcooled boiling region is negligibly small in comparison to the saturated boiling region. Axial elevations of interest are the two-phase mixture level, assumed to be coincident with the fuel rod dryout point, and the collapsed liquid level, the elevation to which liquid would fall if boiling ceased. In the interest of generality, the datum of the system is defined as the elevation where saturated boiling begins.

Two-phase mixture level swell is defined as the relative vertical expansion of a two-phase region due to the presence of vapor voids. Mathematically, mixture swell is defined as

$$S = \frac{Z_{mix} - Z_{CLL}}{Z_{CLL}} \quad , \tag{1}$$

where all elevations are referenced to the elevation where saturated boiling begins. In addition, mixture level swell can be expressed as a function of local void fraction

$$S = \frac{Z_{mix}}{\int_0^{Z_{mix}} [1 - \alpha(Z)]dz} - 1.0 \quad . \tag{2}$$

Mixture level swell is of importance in the study of small break accidents because, for a given geometry and coolant loss, the mixture swell directly affects the amount of core that remains covered. Mathematically this is illustrated by rearranging Eq. (1) and noting that the coolant inventory in the boiling length is given by

$$M = \rho_f A_F Z_{CLL} \quad . \tag{3}$$

The result shows the mixture level to be directly related to the mixture swell

$$Z_{mix} = \frac{M}{\rho_f A_F} (S + 1) \quad . \tag{4}$$

It was the objective of the subject test series to characterize both mixture level swell and axial void fraction distribution under conditions of varying pressure and heat flux.

Experimental Procedures

Experimental testing was performed in the Thermal Hydraulic Test Facility (THTF), located at ORNL (Ref. 1). The THTF is a high pressure test loop containing a 3.66-m, 8 x 8 electrically heated rod bundle (Fig. 2). The axial power profile is uniform and bundle configuration is typical of a Westinghouse 17 x 17 fuel assembly. The fuel rod simulator (FRS) bundle is instrumented with FRS sheath thermocouples at 25 elevations. Most of the FRS thermocouple "levels" are in the upper 30% of the bundle. This allows the determination of dryout elevation to within ± 0.08 m. Axial void fraction distributions were determined from the outputs of a set of stacked differential pressure cells (Fig. 3,.* Because of the low liquid and vapor velocities extant in these tests, friction and form pressure drops are negligible and the differential pressure cell output is directly related to the hydrostatic head of the liquid and steam between the instrument taps. Then, as described in the appendix, the hydrostatic head can be used to compute a volume average void fraction.

The experimental procedure used in these tests was designed to allow the acquisition of void distribution data under quasi-steady-state conditions. The test began by preheating the THTF to the desired test section inlet temperature, reducing inlet flow to the desired value and applying bundle power. The flow-power combination was such that most of the heated length would experience saturated boiling and only the uppermost portion of the core would experience dryout. After a period of stabilization the test section flow was trimmed to place the mixture level in the uppermost 0.6 m of heated length. Finally, when the system had stabilized and makeup flow was just sufficient to compensate for liquid being vaporized, quasi-steady-state data was taken.

*PdE-189 failed prior to testing.

Primary measured quantities include: (1) system pressure, (2) FRS current and voltage, (3) test section inlet and outlet volumetric flows and temperatures, (4) FRS axial temperature profile, and (5) test section differential pressure profile.

Presentation and Discussion of Results

A total of 17 mixture swell and void distribution tests have been run. Eight of the tests were run at approximately 4.0 MPa and nine tests at about 8.0 MPa. Tests at four different linear power levels, ranging from 0.33 to 1.95 kW/m, were run at each pressure. Table 1 summarizes test conditions and calculated mixture swell for each test. In addition, Table 1 presents mixture swell results from a series of small break heat transfer tests run in January of 1980 (Ref. 2). Test procedure and differential pressure instrumentation were different in the January 1980 tests. As such, the test data are an indicator of the experimental repeatability of the mixture swell results.

Table 1 indicates that, for several tests, the two-phase mixture level was at or just above the upper end of the heated length. Although this does not affect local void fraction measurements, it does affect the calculated mixture swell. As such mixture swell data from tests with mixture levels at or above 3.66 m should be used with caution.

Mixture Level Swell

A systematic study was undertaken to determine if mixture level swell could be correlated against any system parameters. The strongest correlating parameter was determined to be the total test section volumetric vapor generation rate. Total volumetric vapor generation rate is based on the measured test section inlet flow

$$\dot{Q} = \frac{\dot{Q}_{in}\rho_{in}}{\rho_g} \quad . \tag{5}$$

In the interest of generality, the volumetric vapor generation rate is divided by the test section flow area. The resulting parameter is, assuming negligible entrainment, the volumetric vapor flux density at the two-phase mixture level.

Figure 4 displays level swell plotted against the vapor flux density at the mixture level. As indicated, mixture level swell is correlated reasonably well with the equation

$$S = 0.0109\, j_{mix} \quad , \tag{6}$$

where it was assumed that mixture swell is zero for zero vapor flux density. The slope of the line was determined by a least squares fit of the data with vapor flux densities < 90 cm/s. Only the lower vapor flux data was used in

Table 1. Summary of mixture level swell test conditions

Small Break Test Series	Linear Power (kW/m)	System Pressure (MPa)	Vapor Flux Density at Mixture Level (cm/s)	Mixture* Level (m)	Collapsed* Liquid Level (m)	Start of* Boiling Length (m)	Mixture Level Swell
I	1.17	2.89	102.9	2.87	1.54	0.24	1.01
I	0.82	4.23	47.8	2.59	1.86	0.34	0.48
I	1.35	4.26	83.2	2.74	1.61	0.30	0.87
I	0.88	7.02	26.6	2.58	2.04	0.27	0.31
I	1.24	6.96	42.3	2.43	1.76	0.30	0.46
I	1.38	2.67	114.5	2.43	1.25	0.21	1.13
II	1.92	4.04	158.8	3.54	1.80	0.60	1.45
II	1.92	4.01	160.0	3.54	1.80	0.60	1.45
II	1.29	4.04	104.0	3.42	2.00	0.56	0.98
II	1.29	4.00	104.8	3.42	1.99	0.55	0.99
II	0.65	3.86	48.7	3.31	2.33	0.48	0.53
II	0.65	3.84	48.7	3.23	2.30	0.46	0.50
II	0.33	3.59	40.0	3.60	2.87	0.41	0.29
II	0.33	3.56	33.3	3.66	2.86	0.42	0.33
II	1.95	8.05	76.5	3.66	2.34	1.02	1.00
II	1.95	7.98	74.1	3.66	2.42	1.03	0.88
II	1.95	7.93	74.4	3.66	2.44	1.02	0.86
II	1.31	7.69	46.6	3.07	2.24	0.83	0.59
II	1.30	8.09	45.9	3.23	2.39	0.90	0.57
II	1.30	8.19	45.2	3.31	2.41	0.93	0.61
II	0.65	7.64	27.2	3.37	2.81	0.88	0.29
II	0.65	7.72	26.9	3.47	2.85	0.92	0.32
II	0.33	7.48	12.3	3.23	2.90	0.86	0.17

*Elevation is with respect to beginning of heated length.

the curve fit because these flux densities are of greatest interest under small break conditions. Data at higher vapor flux densities appear to have a somewhat shallower slope than the lower vapor flux data. This is consistent with test results from the THETIS facility at Winfrith. Shires, Pearson, and Richards have found that at high pressure the mixture swell tends toward a limiting maximum value as linear power is increased (Ref. 3).

The significance of these results can be understood through a simple parametric study. A statement of the problem is as follows:

> Given that a nuclear reactor is undergoing a slow, small break loss of coolant accident, what fraction of initial active core coolant inventory is required to assure that uncovering of active core does not occur. Assumptions and conditions that apply are:
>
> a) Mixture swell is characterized by Eq. (6)
> b) System pressure is 6.9 MPa
> c) Vapor generation by flashing is small compared to that by heat addition
> d) Heat losses are negligible
> e) Entire active core is in saturated boiling
> f) ANS decay curve characterizes decay heat levels
> g) Calculations are based on a 0.95-cm-diam fuel rod and a pitch-to-diameter ratio of 1.34
> h) Decay heat based initial power of 18.4 kW/m

Results of the study are displayed in Fig. 5. Time is defined with respect to reactor SCRAM. The study indicates that in the time period of primary interest in small break accidents, 1000 to 10,000 s after SCRAM, roughly 80 to 90% of the active core liquid inventory is required to maintain core coverage. Also plotted in Fig. 5 is the increase in mixture level due to level swell.

Figure 4 indicates that the level swell for the 8.0 MPa data is somewhat higher than the 4.0 MPa and Small Break Test Series I data for conditions of similar vapor flux density. It is reasonable to ask what effect this difference might have on the parametric study results. A line passing through the origin and bounding the 8.0 MPa data has a slope of 0.0132/(cm/s). The differences in mass inventory needed to maintain core coverage that result from differences in slope are quite small for times greater than or equal to 1000 s. Figure 5 shows that 88% of initial active core liquid inventory is needed to maintain core coverage at 10,000 s. If the slope is changed to 0.0132/(cm/s) the result is 86%. So while pressure may have affected the amount of level swell at a given vapor flux density, the calculated differences in core behavior were insignificant for the time period of interest.

Despite the attractive simplicity of these results, they should not be taken too literally. Recall that the THTF has an axially uniform power profile. It is not known what effect, if any, the nonuniform power profile of an operating reactor might have on level swell. However, these calculations should approximate the dependency of mixture swell on decay heat level. In addition, the calculations form a basis for more detailed studies.

Local Void Fraction Data

Void Fraction Distribution

Local void fraction distributions are plotted for the 4 MPa data base, Fig. 6, and the 8 MPa data base, Fig. 7. Each plot is composed of the data from four selected tests, one test for each linear power level. Data points are plotted at the midpoint between the respective differential pressure cell taps. All elevations are with respect to the beginning of heated length.

Figure 6 shows that in all 4-MPa tests the void fraction is zero at the first differential pressure cell. This is expected since the inlet flow is subcooled. In the two-phase region, void fraction increases with increasing elevation and the 4-MPa distribution curves for 1.92 and 1.29 kW/m are concave downward. The 0.33 kW/m curve does not show a concave downward distribution, instead the void fraction increase is relatively linear with increasing elevation. The 4-MPa curves show a clear trend of increasing test section average void fraction with increasing power level. This is expected as mixture level swell was observed to increase with increasing power level. The 0.65 and 1.29 kW/m distributions show a sharp increase in void fraction at or near the mixture level. The mixture level was slightly above the uppermost functioning differential pressure cell tap in the 1.92 and 0.33 kW/m tests. As a result, sharp increases in void fraction were not observed in these tests.

The 8-MPa distribution curves in Fig. 7 appear considerably different than the 4-MPa curves. None of the curves have a concave downward shape and, in fact, the 0.33 and 0.65 kW/m curves appear slightly concave upward. In addition, the increase in test section average void fraction with increasing power level is not as great as in the 4-MPa data base. The reason is that the vapor density increases with pressure. Therefore, the increase in the volumetric vapor generation rate for a given increase in power is less in a high pressure test as compared to a lower pressure test. The mixture swell data showed that a smaller increase in the vapor generation rate translated into a smaller increase in average void fraction. The result is that the 8-MPa void distributions are not as sensitive to changes in power as the 4-MPa distributions.

A detailed analysis of the void distribution data is beyond the scope of this paper. However, some of the trends in the data may be explained through the use of a drift-flux model for local void fraction (ref. 4),

$$\langle\alpha\rangle = \frac{\langle j_g \rangle}{C_o \langle j \rangle + V_{gj}} \quad , \tag{7}$$

where the brackets signify an area average. If it is assumed that $C_o = 1.0$, Eq. (7) can be written in terms of the void fraction if there was no slip between phases,

$$\langle\alpha\rangle = \frac{\langle\alpha\rangle_o}{1 + V_{gj}/\langle j\rangle} \quad , \tag{8}$$

where $\langle\alpha\rangle_o = \langle j_g\rangle/\langle j\rangle$ is the no slip void fraction.

The no slip void fraction increases rapidly with quality and approaches 1.0 at moderate qualities. For example, the no slip void fraction at a quality of 0.3 and pressure of 8 MPa is 0.88. The denominator in Eq. (8) always reduces the void fraction from the no slip case. If, for a given pressure and flow regime, the mean-weighted drift-velocity is relatively constant, then the denominator increases with decreasing bundle power. The reason is that, for a given quality, total volumetric flux density increases with power. The result is that the rate of increase in void fraction with elevation should decrease with decreasing power level. The data in Figs. 6 and 7 seem to verify this.

At moderate to high quality $\langle\alpha\rangle_o \approx 1.0$ and $\langle j\rangle \approx xj_{mix}$. Equation (8) can thus be written as

$$\langle\alpha\rangle \approx \frac{1}{1 + V_{gj}/xj_{mix}} \quad . \tag{9}$$

Equation (9) shows that, for a given value of V_{gj}, there is a limiting value of void fraction, which is attained when $x = 1.0$. This limiting void fraction increases with power because j_{mix} increases with power. A way to exceed this limit is to change V_{gj} and thus flow regime. The data in Figs. 6 and 7 seem to show this trend. Generally void fraction increases in a relatively linear fashion over most of the heated length. However, at some elevation, below the mixture level, there is a sharp increase in void fraction which terminates in dryout. The best examples of this are the 0.65 kW/m distribution in Fig. 6 and the 0.33 and 1.31 kW/m distributions in Fig. 7. It is thought that this sharp increase in void fraction is caused by a flow transition. The void fraction at which the transition occurs decreases with decreasing j_{mix}, as might be expected from Eq. (9).

It is interesting to note that all the observed flow regime transitions appear to occur at roughly the same elevation. Because the boiling length in each of the tests was roughly equal, it is implied that the flow transitions are quality dependent.

The final observation is that Eq. (9) asymptotically approaches 1.0 as j_{mix} goes to infinity. Thus, it might be expected that the high flux density void distributions in Fig. 6 would be slightly concave downward, as they are. The result is a reduction in mixture level swell when compared to a linear void distribution. This may account for the reduction in the slope of mixture swell with respect to vapor flux density that was observed at high j_{mix}.

Mean Velocity vs Flux Density Plots

The drift-flux model expresses void fraction in terms of a concentration parameter C_0 and a mean-weighted drift-velocity V_{gj}. Generally these quantities are determined from experimental data. Rearrangement of Eq. (7) yields

$$\langle j_g \rangle / \langle \alpha \rangle = C_0 \langle j \rangle + V_{gj} \quad , \tag{10}$$

where $\langle j_g \rangle / \langle \alpha \rangle$ is the mean vapor velocity. It is clear from Eq. (10) that, for a system in which void fraction can be expressed in terms of Eq. (7), C_0 and V_{gj} can be derived from a plot of local void fraction data in the mean-velocity, flux density plane. The concentration parameter is the slope of the mean-velocity with respect to flux density and V_{gj} is simply the zero flux density intercept of the data.

Figures 8 and 9 are the mean-velocity vs flux density plots for the 4- and 8-MPa data sets respectively. Void fraction is derived as a volume average quantity and the vapor and mixture flux densities are evaluated at the midpoint between the differential pressure cell taps.

Most of the data in Fig. 8 is fit reasonably well by the line

$$\langle j_g \rangle / \langle \alpha \rangle = 0.91 \langle j \rangle + 0.478 \quad ,$$

where the mean-velocity is in m/s. However, the 0.33 kW/m and, to some extent, the 0.65 kW/m data are not fit very well. There are a number of reasons why this is the case. First, low power tests are characterized by low void fractions over most of the heated length. Errors inherent in void fraction measurements can be magnified when propagated through the ratio $\langle j_g \rangle / \langle \alpha \rangle$. This is particularly so when void fraction is low. Therefore, the large scatter in the low power data may be due, at least in part, to uncertainties in experimental measurements. A second possibility is that a drift-flux model with a constant drift velocity and concentration parameter may not be sufficiently accurate under very low power conditions. In either case, further work is recommended as low power level data is of prime importance under small break conditions.

The 8-MPa data in Fig. 9 shows some scatter but is fit reasonably well by the line

$$\frac{\langle j_g \rangle}{\langle \alpha \rangle} = 0.85 \langle j \rangle + 0.338 \quad .$$

This indicates a pressure dependency of both the mean weighted drift-velocity and concentration parameter. Close examination of Fig. 9 shows that, as with the 4-MPa data, considerable scatter exists at low power levels (0.33 kW/m).

The drift-velocities and concentration parameters that have been calculated are the result of arbitrarily fitting a line to the composite of all data at a given pressure. As such they do not reflect a detailed understanding of the flow phenomena extant in these tests. However, the derived drift-velocities and concentration parameters are consistent in the sense that the resulting drift-flux models predict void fraction profiles that are in reasonable agreement with those in Figs. 6 and 7.

Conclusions

Mixture level swell was determined to be directly proportional to the total volumetric vapor generation rate over the range of power and pressure of interest in small break analysis. A simple parametric study, based on the level swell data, indicated that 80 to 90% of initial active core liquid inventory was required to assure active core coverage in the interval 1000 to 10,000 s after reactor SCRAM; pressure was assumed 6.9 MPa.

Axial void fraction profiles, at a given pressure, show an increase in core average void fraction with increasing power. General trends in the data can be explained through the use of a drift-flux model and flow regime transitions appear governed by equilibrium quality. When the void fraction data is plotted in the mean-velocity, flux density plane a concentration parameter and mean-weighted drift-velocity can be derived for the 4- and 8-MPa data sets. Both concentration parameter and mean-weighted drift-velocity were observed to decrease with increasing pressure. Very low power void fraction data did not conform well to a simple drift-flux model.

Acknowledgments

The authors wish to express their appreciation to M. S. Thompson for her help in preparation of this paper and to D. K. Felde for his skillful operation of the THTF.

Literature Cited

1. Felde, D. K., Project Description–ORNL PWR Blowdown Heat Transfer Separate Effects Program-Thermal Hydraulic Test Facility (THTF) Mod 3, ORNL/TM-7842.

2. Anklam, T. M., ORNL Small Break LOCA Heat Transfer Test Series I: Two-Phase Mixture Level Swell Results, ORNL/NUREG/TM-447, 1981.

3. Shires, G. L., Pearson, K. G., and Richards, A. D., An Experimental Study of Level Swell in a Partially Water Filled Fuel Cluster, Nucl. Energy, Vol. 19, 1980.

4. Zuber, N. and Findlay, J. A., Average Volumetric Concentration in Two-Phase Flow Systems, ASME Journal of Heat Transfer, Vol. 87.

Nomenclature

A_f Bundle flow area

C_o Concentration parameter

G Mass flux

j Volumetric flux density

M Mass

M_o Initial active core mass inventory

$\dot{Q}$ Volumetric flow

S Mixture level swell

V_{gj} Mean-weighted drift-velocity

X Quality

Z Elevation

α Void fraction

ρ Density

Subscripts

CLL Collapsed liquid level

f Saturated liquid

g Saturated vapor

in Inlet

mix Mixture level

o No slip between phases

sat Start of saturated boiling

Appendix

The volume average void fraction is defined in terms of the mixture density, which is deduced directly from the differential pressure cell reading. Mixture density is defined as

$$\bar{\rho} = \alpha\rho_g + (1 - \alpha)\rho_f \quad ,$$

where α is volume average void fraction, ρ_f is saturated liquid density and ρ_g is saturated vapor density. Rearrangement of the mixture density relationship yields

$$\alpha = \frac{\rho_f - \rho}{\rho_f - \rho_g} \quad .$$

The vapor and liquid mean flux densities are related to the mixture quality x and system mass flux G.

$$\langle j_g \rangle = xG/\rho_g$$

$$\langle j_f \rangle = [(1 - x)G]/\rho_f$$

$$\langle j \rangle = \langle j_g \rangle + \langle j_f \rangle$$

As the THTF power profile is uniform, x can be calculated from a linear interpolation

$$x = \frac{Z - Z_{sat}}{Z_{mix} - Z_{sat}} \quad .$$

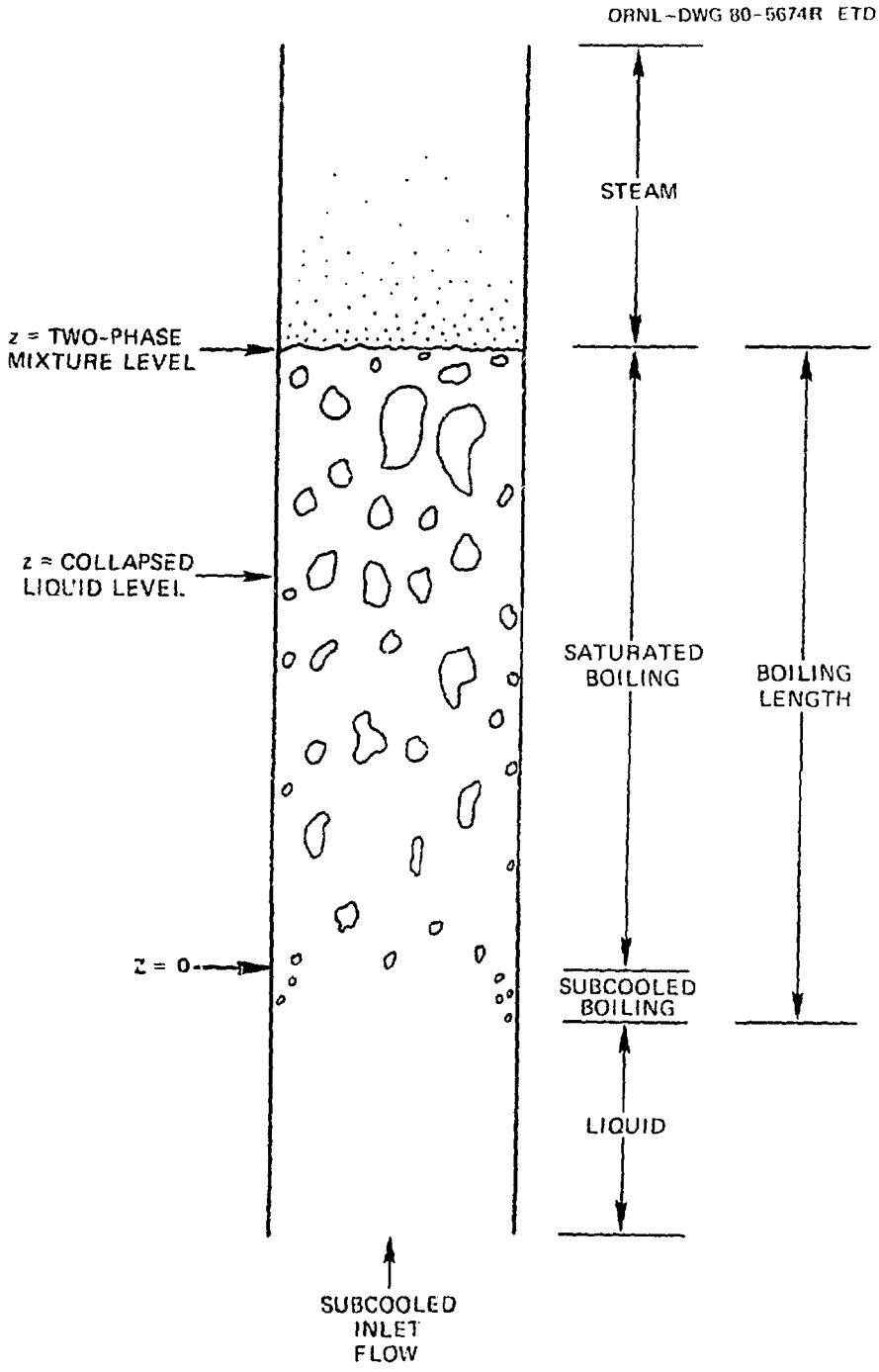

Fig. 1. Schematic of nuclear reactor subchannel in a partially uncovered configuration.

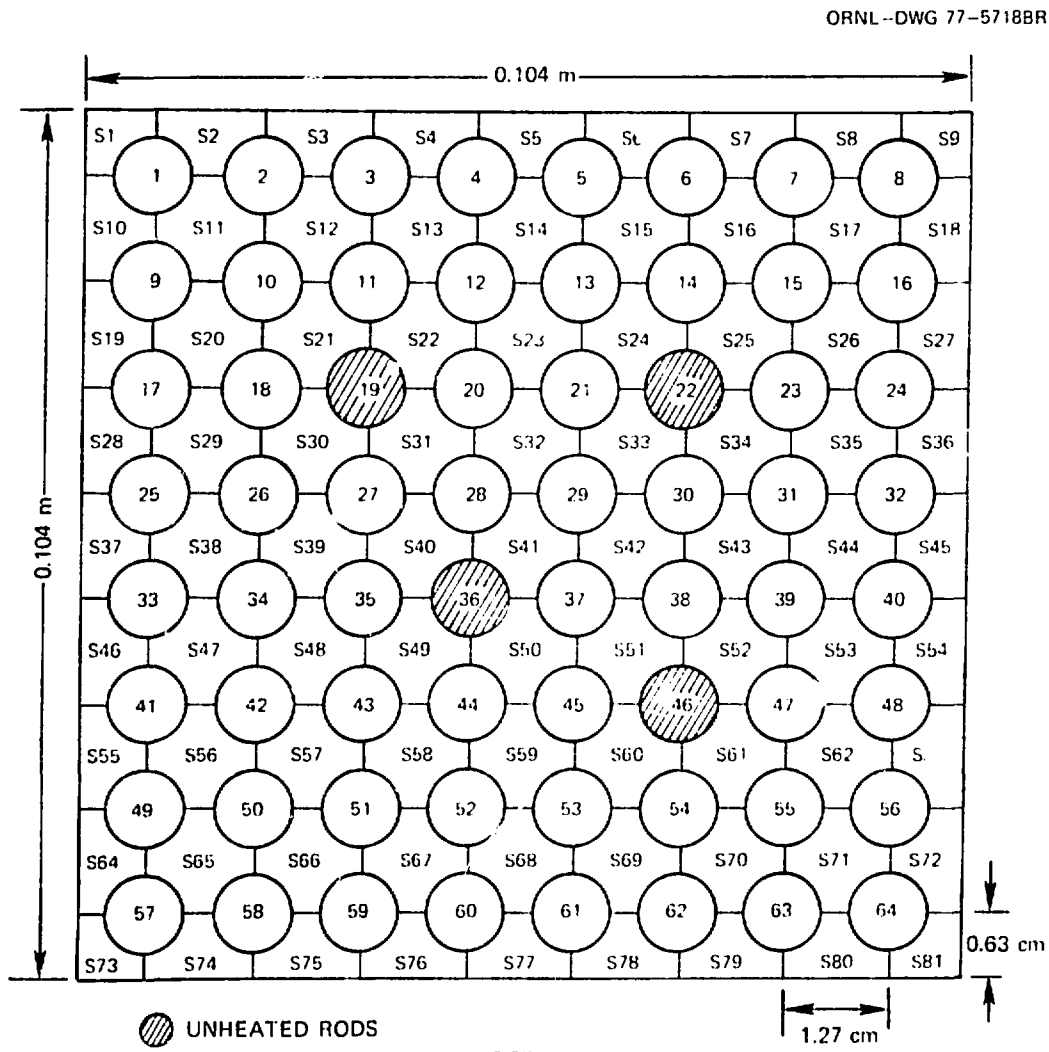

Fig. 2. Cross section of THTF bundle 3.

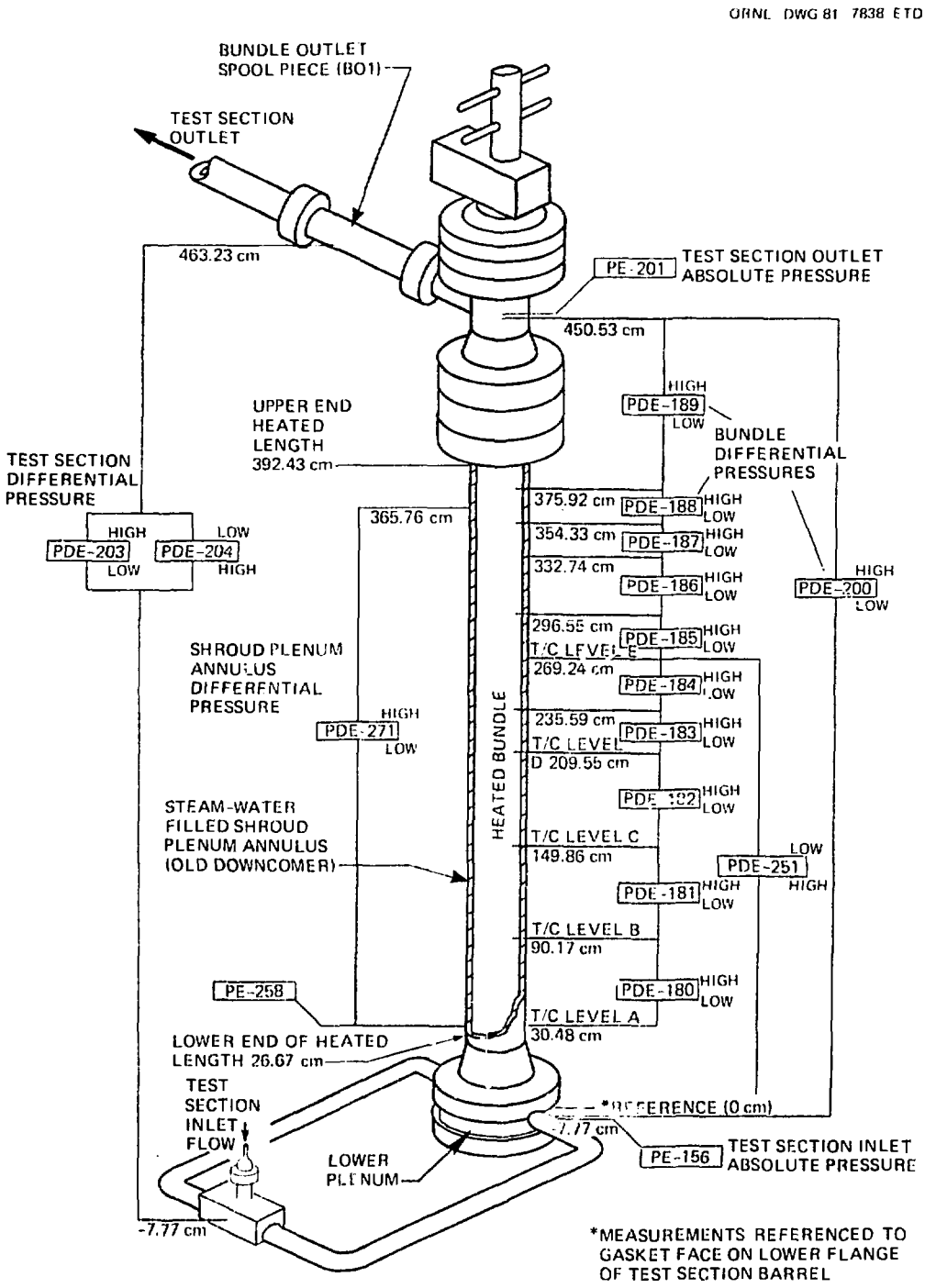

Fig. 3. THTF in-bundle pressure instrumentation; all elevations referenced with respect to gasket face on lower flange of test section barrel.

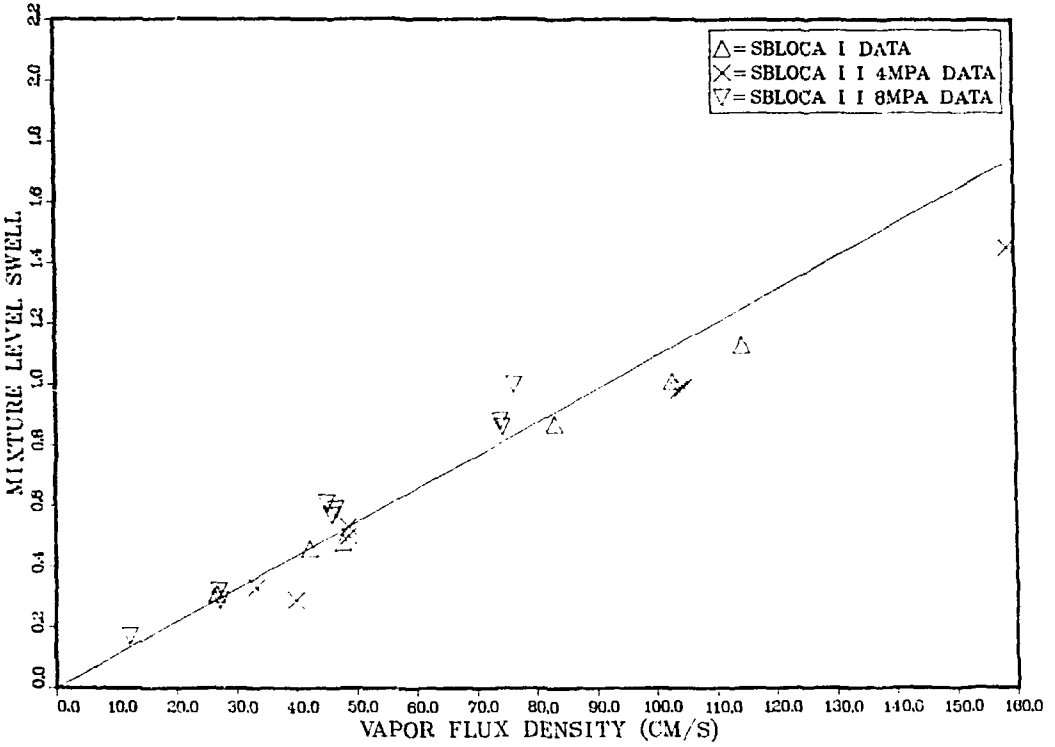

Fig. 4. Two-phase mixture level swell vs volumetric vapor flux density evaluated at two-phase mixture level; line represents $S = 0.0109\ j_{mix}$.

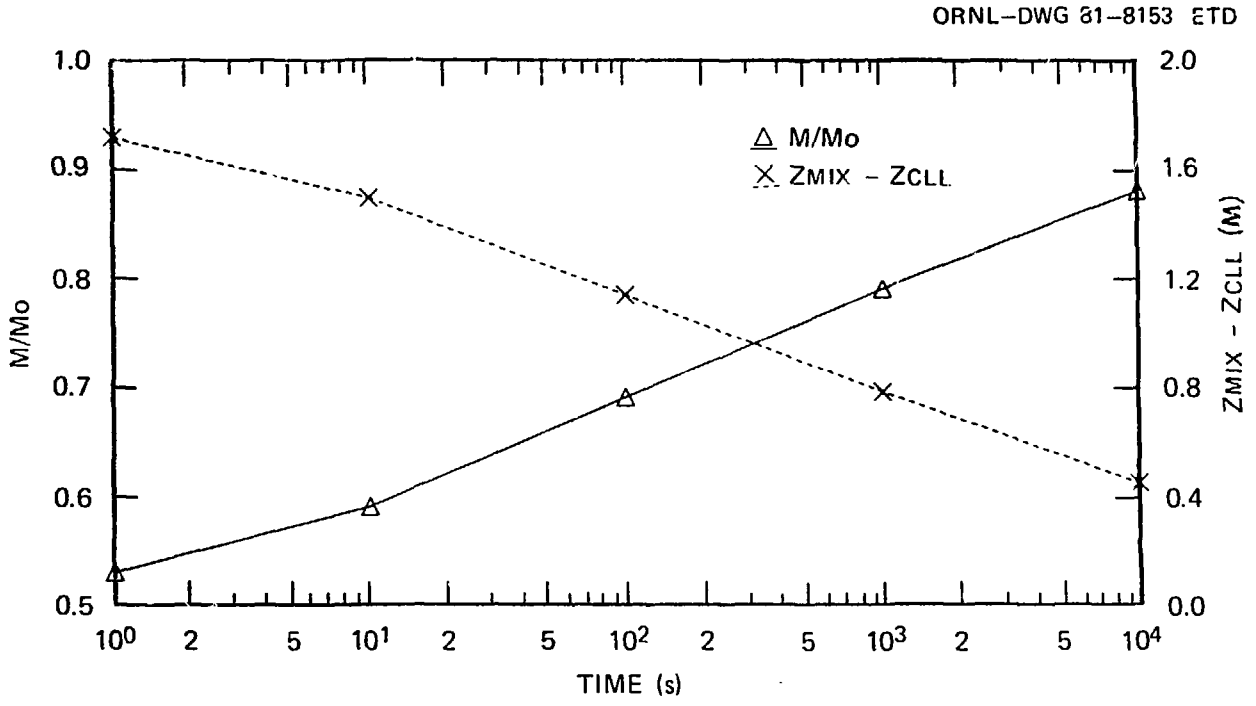

Fig. 5. Fraction of initial active core liquid inventory required to assure core coverage and increase in mixture level resulting from mixture level swell vs time after reactor SCRAM.

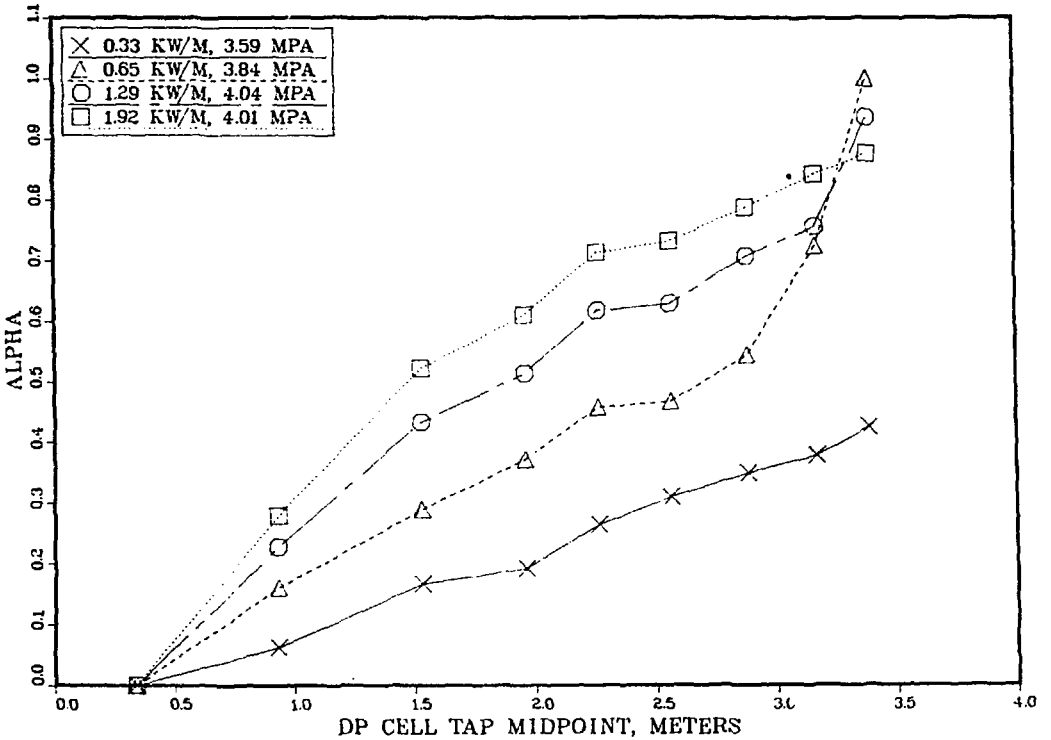

Fig. 6. Axial void fraction profiles for 4-MPa data set.

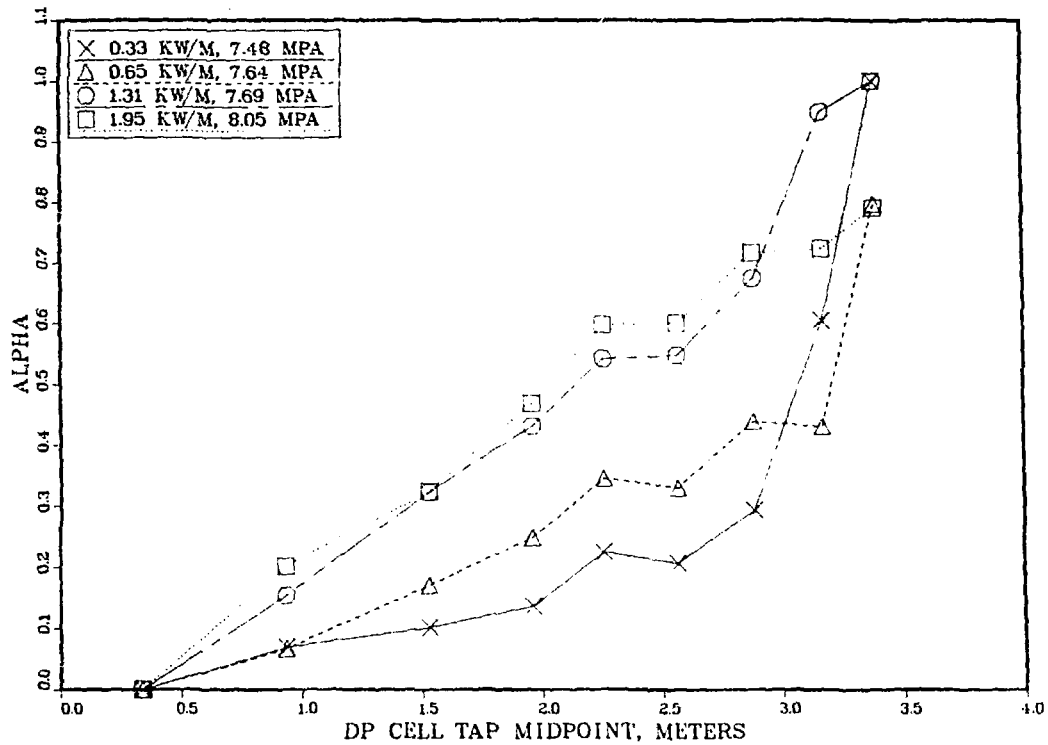

Fig. 7. Axial void fraction profiles for 8-MPa data set.

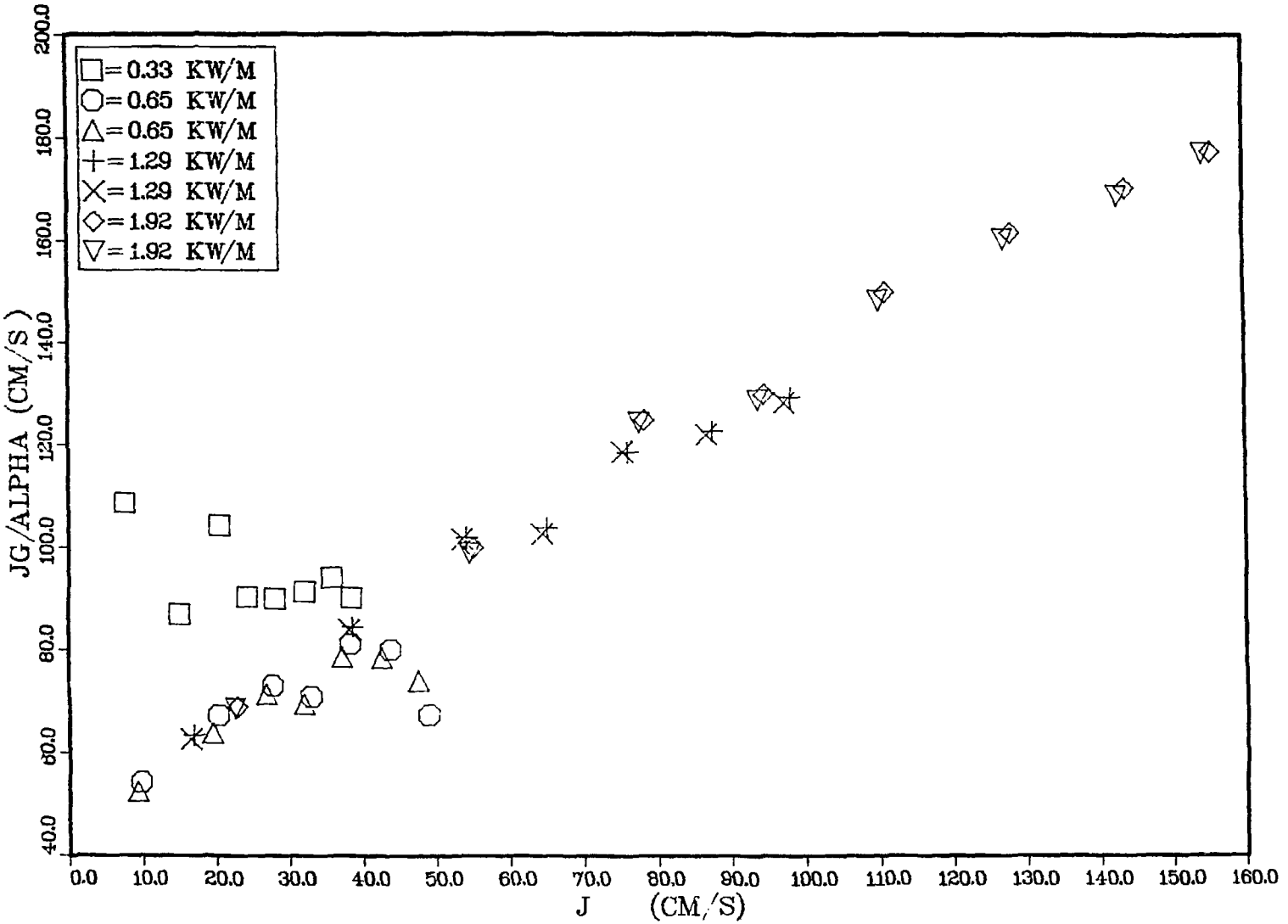

Fig. 8. Mean-velocity vs flux density plot for 4-MPa data set.

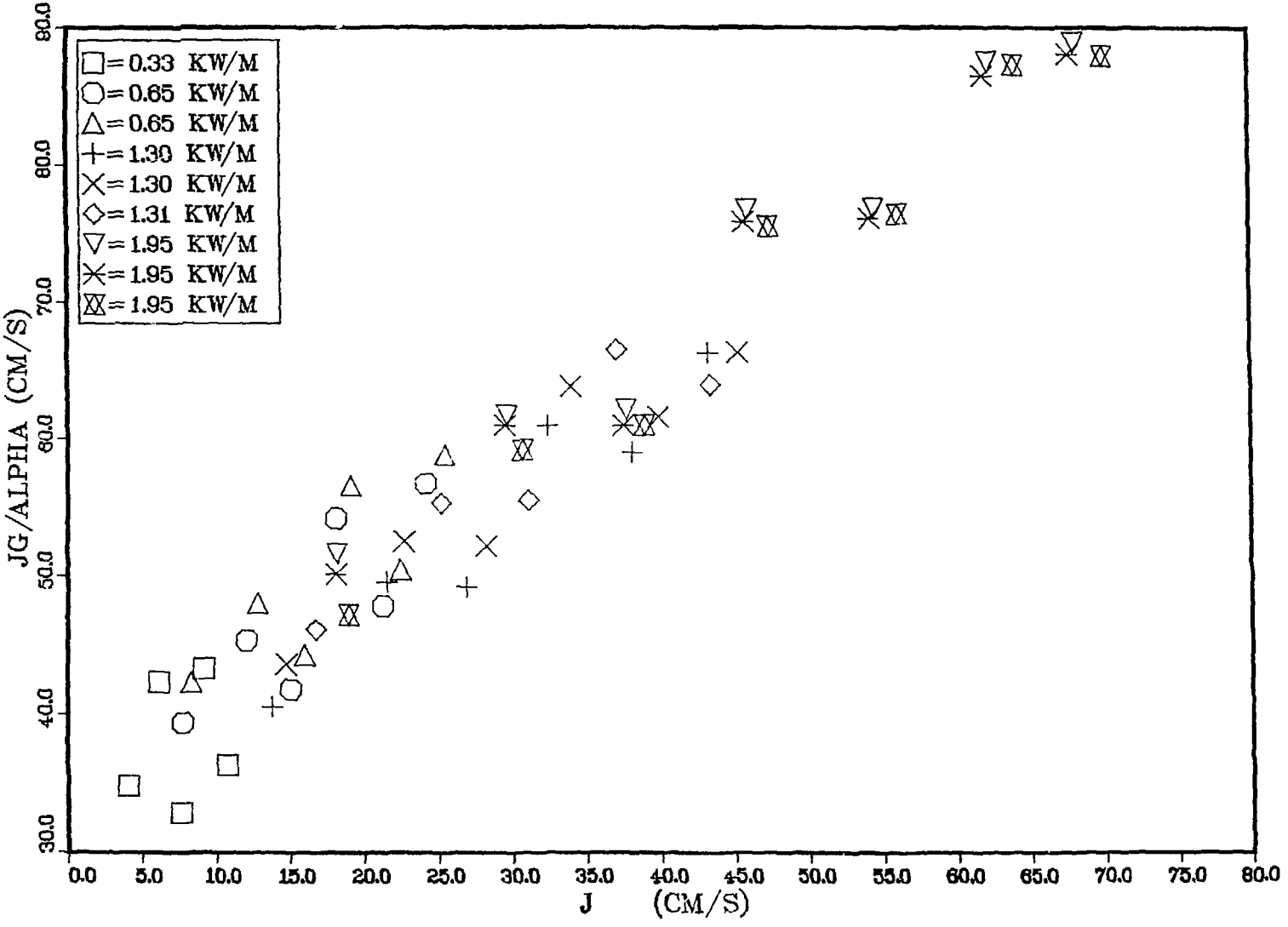

Fig. 9. Mean-velocity vs flux density plot for 8-MPa data set.